Treatment of diabetic foot ulcers with Therapeutic Magnetic Resonance (TMR®) improves the quality of granulation tissue

Letizia Ferroni,[1] Chiara Gardin,[1] Andrea De Pieri,[1] Maria Sambataro,[2] Elena Seganfreddo,[2] Elisabetta Iacopi,[3] Chiara Goretti,[3] Barbara Zavan,[1] Alberto Piaggesi[3]

[1]**Department of Biomedical Sciences, University of Padua**
[2]**Metabolism Disease and Clinical Nutrition Unit, Santa Maria di Ca' Foncello Hospital, Treviso**
[3]**Department of Medicine, University of Pisa, Italy**

Abstract

Diabetic foot ulcers (DFUs) often result in severely adverse outcomes, such as serious infections, hospitalization, and lower extremity amputations. In last few years, to improve the outcome of DFUs, clinicians and researchers put their attention on the application of low intensity pulsating electro-magnetic fields through Therapeutic Magnetic Resonance (TMR®). In our study, patients with DFUs have been divided into two groups: The Sham Group treated with non-functioning TMR® device, and the Active Group treated with a functioning device. Biopsies were recovered from ulcers before and after a 15-day treatment with both kind of TMR® device. To recognize signs of inflammation or healing process, the harvested biopsies were subjected to histological and molecular analyses. The histological analysis showed a change in cell population after treatment with TMR®: an increase of fibroblasts and endothelial cells with a reduction of inflammatory cells. After TMR® application, the gene expression profile analysis revealed an improvement in extracellular matrix components such as matrix metalloproteinases, collagens and integrins, a reduction in pro-inflammatory interleukins, and an increase in growth factors expression. In conclusion, our research has identified histological and molecular features of reduced inflammation and increased cell proliferation during the wound healing process in response to TMR® application.

Introduction

Diabetes mellitus causes chronic hyperglycemia and a wide range of downstream metabolic disturbances and multi-organ complications.[1] The most prevalent form of this disease is Type 2 diabetes mellitus, recently recognized as a group of metabolic disorders. It predisposes to lower extremities ulceration and impairs the healing process leading to wound chronicity.[2] Indeed, insulin deficiency predisposes to inflammation, that hampers proliferation, migration, homing, and organization of fibroblasts and endothelial cells to produce a granulation tissue.[3] Wound healing is a complex process that involves different cell types and molecules, which operate in coordination to repair and regenerate tissue. They also produce and secrete large amounts of reactive oxygen species (ROS), which are essential to protect the organism against invading bacteria and other microorganisms. However, excessive and persistent production of ROS is harmful as this leads to a delay and impairment of the healing process.[4] The healing process in diabetic patients is compromised giving rise to chronic wounds that do not heal. Diabetic foot ulcers (DFUs) often result in severely adverse outcomes, such as serious infections, the need for hospitalization and lower extremity amputations, that are associated with a five-year mortality around 50%.[5,6] Treatments for DFUs include surgical debridement and drainage, antimicrobial therapy for infected wounds, pressure off-loading methods and advanced wound dressings.[7] Despite these treatments, lower extremity amputations in diabetic patients occur at a rate 17 to 40-fold higher than in non-diabetic individuals.[8,9] Thus, many clinicians and researchers have made efforts to develop adjunctive or complementary treatments to improve the outcome of DFUs. In last few years, lot of attention has been put on physical based treatment such as the application of low intensity Pulsating Electro-Magnetic Fields (PEMFs). The application of PEMFs has been successfully introduced in a number of conditions ranging from to neurology rehabilitation to tissue repair, with generally positive results.[10-12] In particular, experiences in clinical settings have confirmed the safety and effectiveness of PEMFs through Therapeutic Magnetic Resonance (TMR®) in promoting tissue repair in post-traumatic and chronic wounds, making this technology potentially interesting for the management of DFUs and post-surgical wounds.[13,14] Furthermore, in an in vitro dermal-like tissue, we have previously demonstrated that TMR® enhances skin wound healing improving the quality of the extracellular matrix (ECM) and reducing ROS, leading to a positive rejuvenation effect on cells.[15] In the present work, we investigated, under clinical, cellular and molecular biology point of view, the influence of PEMFs on wound healing process in consecutive Type-2 diabetic patients, studying the granulation tissue of DFUs treated with TMR®.

Materials and Methods

Patients recruitment

The study was conducted according to ethical principles for medical research involving human subjects of world medical association declaration of Helsinki. The selected patients agreed to participate to the study by signing a consent form previously approved by the Institutional Ethics Committee of University of Pisa (Italy) and Local Ethics Committee of the Treviso Province. Before starting the study a letter was sent to their GPs informing them about the characteristics of the study in which the patient was included.

In a subset of 40 patients participating in a multicenter clinical trial (No 3593/2012; University of Pisa and Ca' Foncello Regional Hospital of Treviso) on the safety and effectiveness of TMR® in the management of DFUs, we analyzed tissue sampling coming from the ulceration before and after the application for two weeks of Sham (Group A; n=20) or Active (Group B; n=20) TMR® device (Thereson Srl, Vimercate, MB, Italy) on top of standard therapy.

Patients were consecutively recruited

among those participating to the aforementioned study according to the following inclusion criteria: older than age 18 years; suffering from Type 2 diabetes lasting for 5 years or more; having a distal neuropathic ulcer to the foot started more than 6 weeks larger than 1 cm^2, involving the dermis at full-thickness; having two palpable pulses at the ankle with a triphasic Doppler waveform. Exclusion criteria were: local ischemia with an ankle-brachial pressure index (ABPI) <0.9; infection according to the Infective Diseases Societies of the Americas (IDSA) guidelines; active or chronic Charcot's disease; cancer; HIV or any other systemic disease interfering with immune system; steroid or cytostatic therapy; presence of pacemaker; pregnancy or fertility state; contralateral amputation; inability to stand and walk alone without aid; life expectancy shorter than 1 year.

Patients in both groups were treated as per standard therapy in each center participating in the study, and Sham (Group A) or Active (Group B) TMR® was added on top.

Patients were followed up to complete healing or up to six months, and healing rate was the primary endpoint of the study; details of the clinical trial in the study by Piaggesi et al.[16]

Patients treatment

According to the International Consensus on the Management of Diabetic Foot's guidelines,[17] the lesions underwent to sharp debridement, eliminating all the visible dead or non-viable tissue, while leaving as intact as possible the living tissue inside and on the edge of the ulcers, opening any eventual sinus or tract, exposing all the wound bed; then the lesions were measured tracing the margins on a polyurethane sheet, and then their area was calculated by means of a VisitrakTM tablet (Smith & Nephew, Hull, UK). The ulcers were also photographed according to the indications of the guidelines for the correct imaging of wounds.[14]

All the procedures were carried out on all patients of both groups in the same way, by expert and trained staff, and the only difference was the inception of TMR® on top of therapy in Group B. All patients received a TMR® device for a daily home therapy of two consecutive weeks: subjects of Group A received a non-functioning TMR® device, whereas subjects of Group B received a functioning TMR® device. The random assignment of devices to patients were warranted by the pre-disposition of the equipment, which was done by the manufacturer before the delivering of devices to the centers. Both patients and investigators were thus blinded to actual treatment which the patients received.

The apparatus for TMR® treatment is configured for generating an electromagnetic wave with specific contribution in frequency that is constituted, as a cascade, by pulses generated at a certain frequency. The TMR® device is composed of a console that generates electrical signals and an emitter connected to the console that converts the electrical signals into PEMFs. The emitter comprises two solenoids with 36 turns of copper wire of 0.8 mm diameter.[13] The signal comprises a plurality of base pulses grouped in pulse packets and in pulse trains, in which each pulse packet consists of a series of base pulses followed by a first pause, in which each pulse train consists of a series of pulse packets followed by a second pause. The control circuit is configured to reverse the polarity of the base pulses after a given time interval. The frequency of the base pulses is varying between 100 and 226 Hz, and the repetition frequency of the pulse packet is 2.89-25.9 Hz. The repetition frequency of pulse trains is 0.3-2.8 Hz, whereas the time interval is 120-180 s. The repetition frequency of the train sets is 0.1-0.3 Hz. The base pulses inside a packet are a sequence of triangular pulses (or better saw tooth) with variable amplitude between 25% and 100% of the maximum gain value. The train of packets is a sequence of base pulses and 'silent' period. The durations of these period ranges between 3 ms and 60 ms. Moreover, the polarity of the signal is inverted during the treatment with variable period between 150 and 300 ms. The therapeutic program is composed of two phases that are repeated twice. Every phase lasts 8 min and it is characterized by different number of base pulses and different duration of pulses, packets and 'frames' (to identify the change of polarity). The average amplitude of the generated magnetic field ranges around 40-60 µT (comparable to the Earth's magnetic field).

The device is composed by a mattress on which the patient lays, containing the solenoids emitting the magnetic field; and a cushion, with another solenoid which, in case of DFUs, is placed in the vicinity of the lesions; both are connected with a computer-controlled generator.

Ulcer sampling

Patients of both experimental groups underwent to sampling by biopsies at baseline and after 15 consecutive days of treatment with TMR®. Biopsies were taken with a scalpel from the edge of the ulcers, removing an oval-shaped sample of 5x10 mm of tissue, involving both the bottom and the margin of the wounds. Both at baseline and after 15 days two equal sampling were taken: one for histology and the other for molecular biology. At baseline biopsies were taken at 12 and 6 h (Figure 1A), respect to the head of the patient; after 15 days of treatment biopsies were taken at 3 and 9 h (Figure 1B). All the biopsies were collected by the same operator (AP) and the margins were closed with a single stitch of nylon 3/0 suture. Harvested biopsies were subjected to histomorphometric and gene expression profile analyses to recognize signs of inflammation or healing process. Biopsies taken at 12 and 3 h were used for histological comparison, while biopsies taken at 6 and 9 h served for biological assays, respectively. After sampling of biopsies, all lesions in both groups were
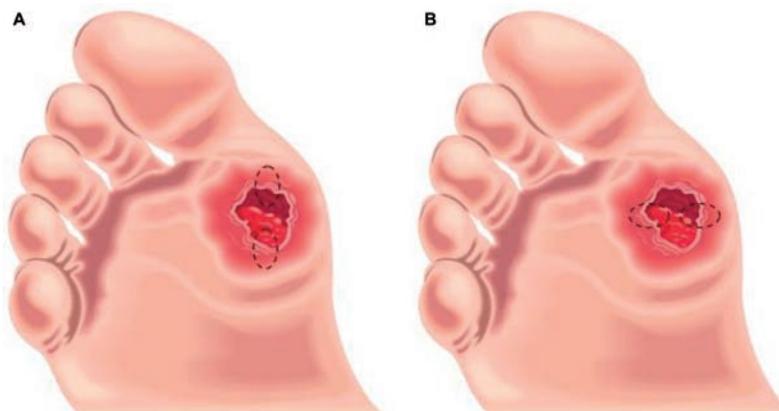

Figure 1. Oval-shaped biopsies of 5x10 mm was taken from the margin of the lesion involving both the edge and the bottom of the ulcer: A) at 12 and 6 h were taken the biopsies at baseline; B) at 3 and 9 h were taken the biopsies after two week of treatment. Samples at 12 and 3 h have been used for histological analysis, while samples at 6 and 9 h for molecular analyses.

dressed with an inert hydrofiber dressing (Aquacel, Convatec, Deeside, UK), according to a previously described procedure,[18] and were offloaded by applying a removable walker (Optima Diab, Molliter, Civitanova Marche, Italy), as previously described.[19]

Histological and histomorphometric analysis

Biopsies were fixed in 4% paraformaldehyde (Sigma-Aldrich, St. Louis, MO, USA) in phosphate-buffered saline (PBS, EuroClone, Milan, Italy) for 24 h, then dehydrated in graded ethanol. After a brief rinse in xylene (Sigma-Aldrich), the samples were paraffin-embedded, and cut into 5-μm-thick sections. Sections were then stained with the nuclear dye hematoxylin (Sigma-Aldrich) and the counter-stain eosin (Sigma-Aldrich). In order to analyze the cellular response of DFUs to treatments, masked microscopic examinations by two researchers were performed, as previously described.[20] Briefly, 3 slides for each sample were analyzed by light microscopy, using 20x as the initial magnification. Each slide contained 3 sections of specimen, and 5 fields were analyzed for each tissue section. A semi quantitative analysis of the presence of the following cell type to compare Group A and Group B were used: i) Polymorphic Nuclear Cells (cells characterized by a nucleus lobed into segments and cytoplasmic granules, *i.e.* granulocytes); ii) phagocytic cells (large mononuclear cells, *i.e.* macrophages and monocyte-derived giant cells); iii) non-phagocytic cells (small mononuclear cells, *i.e.* lymphocytes, plasma cells and mast cells.); iv) fibroblasts; v) endothelial cells; vi) keratinocyte; vii) collagen fibers. All of these items were evaluated blindly and scored as absent (score 0), scarcely present (score 1), present (score 2), and abundantly present (score 3). Experiments were performed at least three times and values were expressed as mean ± SD.

Realtime PCR array analysis

Total RNA from biopsies was extracted with the RNeasy Mini Kit (Qiagen Gmbh, Hilden, Germany), including DNase digestion with the RNase-Free DNase Set (Qiagen), according to the manufacture procedures. RNA samples were checked for concentration and quality using the NanoDrop 1000 Spectrophotometer (Thermo Fisher Scientific, Waltham, MA, USA). The ratio of samples absorbance at 260 and 280 nm were around 2.0 indicating the absence of contaminants such as protein, phenol or other contaminants that

absorb at or near 280 nm. The ratio 260/230 of samples absorbance at 260 and 230 nm were calculated in the range of 1.8-2.2 confirming the purity of the RNA samples. The integrity of the samples was assessed by running an aliquot of RNA samples on a denaturing agarose gel stained with ethidium bromide. The RNA samples were stored at -80°C until the use.

Eight-hundred ng of total RNA of each sample was reverse transcribed with a RT[2] First Strand kit (Qiagen Sciences, Germantown, MD, USA) following the manufacture procedures. Briefly, the procedure includes the elimination of contaminating genomic DNA with a proprietary procedure from RNA samples before the reverse transcription. Then a mix of random hexamers, oligo-dT primers and reverse transcriptase enzyme is used to synthesize cDNA products with optimal yield and length. The reverse transcription reactions were performed in a LifePro Thermal Cycler (Bioer Technology, China) following the manufacture conditions: 42°C for 15 min exactly and 95°C for 5 min (inactivation). The resultant cDNA samples were stored at -20°C until the next use.

Real-time PCR of genes involved in wound healing process were investigated by the Human Wound Healing RT[2] Profiler PCR array (SABiosciences, Frederick, MD, USA) according to the manufacture procedures. This system requires the use of RT[2] SYBR Green ROX FAST Mastermix (SABiosciences) that contains a high-performance HotStart DNA Taq polymerase, nucleotides, SYBR Green dye, and the ROX reference dye needed to normalize the instruments' optics. The chemically-modified Taq polymerase provides accurate results by preventing the amplification of primer dimers and other non-specific products. The real time PCR program was in accord to RT[2] Profiler PCR array instruc-

tions and sets as follow: initial HotStart DNA Taq polymerase activation at 95°C for 10 min; 40 cycles of denaturation at 95°C for 15 s followed by annealing and extension at 60°C for 30 s. Thermal cycling and fluorescence detection during the extension step were performed using a Rotor-Gene Q 100 (Qiagen). The data were analyzed using Excel-based PCR Array Data Analysis templates (SABiosciences). The results are reported as expression of each target gene in post-treatment samples compared to pre-treatment samples in both Group A and Group B.

Statistical analysis

One-way analysis of variance (ANOVA) was used for the data analyses. Levene's test was used to demonstrate equal variance in the variables. Repeated-measures ANOVA with *post-hoc* analysis using Bonferroni's multiple comparison was performed. A *t*-test was used to determine significant differences ($P<0.05$). Repeatability was calculated as the standard deviation of the difference between measurements. All testing was performed in SPSS 16.0 software (SPSS Inc., Chicago, Illinois, USA) (license of the University of Padua, Italy).

Results

Clinical analysis

Forty consecutive patients were comprehensively enrolled in the study and randomized into the two groups: 20 in Group A and 20 in Group B, respectively. In Table 1 are reported the clinical characteristics of patients of each group. All patients completed the study and no drop out was observed in both groups.

From a clinical point of view, no adverse events were reported in any patients

Table 1. Clinical characteristics of the patients participating in the study.

	Group A	Group B
Number of patients	20	20
Age (yrs)	64.7±18.4	65.2±16.7
Duration of diabetes (yrs)	18.5±6.3	17.9±7.1
Glycated haemoglobin (%)	7.9±1.1	8.3±1.8
Insulin/oral hypoglicemic drugs	14/6	15/5
Statins (Y/N)	16/4	18/2
Acetilsalicilic acid (Y/N)	18/2	19/1
Retinopathy (background/proliferative)	17/3	19/1
Albuminuria (micro/macro)	18/2	18/2
Hypertension (Y/N)	16/4	17/3

in both groups during the whole course of the follow-up. During the follow-up, significantly more lesions healed in the Active Group (14/20 in Group B *vs* 4/20 in Group A, P<0.05). Moreover, the healing time was faster in Active Group than in Sham group (44.8±12.1 *vs* 96.7±23.5 days, respectively, P<0.05).

Histological and histomorphometric analysis

A histological analysis of the biopsies harvested from the edge of the same ulcer were performed at baseline and after 15 consecutive days of treatment with TMR® devices. The hematoxylin and eosin staining of all biopsies recovered before whatever treatment with TMR® reveals typical histological features of not-healed tissue, both in Sham Group (Figure 2A) and in Active Group (Figure 2B). On the contrary, a histological overview of the biopsies after the treatment with the two kind of TMR® devices showed different characteristics: UDFs treated with non-functioning TMR® device (Sham group) showed again signs of inflammation (Figure 2C), instead biopsies of Active Group harvested after 15 days of treatment showed signs of wound healing (Figure 2D). A deeper investigation of the biopsies was performed through a histomorphometric analysis that assessed the presence of polymorphic nuclear cells (*i.e.,* granulocytes), phagocytic cells (*i.e,*. macrophages), non-phagocytic cells (*i.e.,* lymphocytes), fibroblasts, endothelial cells, keratinocytes, or collagen fibers (Figures 3 and 4). Before treatment with both kinds of TMR® devices high infiltration of granulocytes and macrophages (red arrows in Figure 3 A,B) were present. In addition, scarce fibroblasts, endothelial cells and keratinocytes, and few collagen fibers were scored both in Sham group (white bars in Figure 4A) and in Active Group (black bar in Figure 4A). After treatment with non-functioning TMR® device, DFUs of Sham Group showed again high infiltration of granulocytes and macrophages (red arrows in Figure 3C; white bars in Figure 4B), scarce fibroblasts, endothelial cells, keratinocytes, and collagen fibers (white bars in Figure 4B). On the contrary, features of healed skin with cells organized into epidermal and dermal tissue compartment were shown in the biopsies of Active Group after the treatment with functioning TMR® device (Figure 3D). A layer of cuboidal epithelial cells with a progressive differentiation of keratinocytes is observed on the surface of the underlying derma (yellow head arrows, Figure 3D). Large amount of collagen fibers (yellow asterisks, Figure 3D),
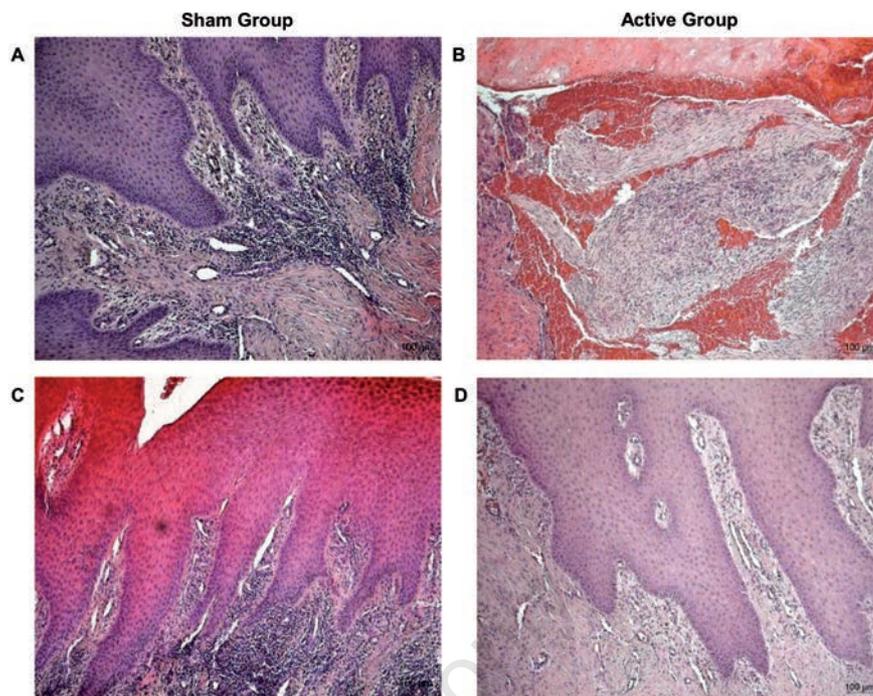

Figure 2. H&E staining of DFUs biopsies of Sham Group and Active Group at 10X magnification: Sham Group at baseline (A) and after the treatment with non-functioning TMR® device (C); Active Group at baseline (B) and after the treatment with functioning TMR® device (D).
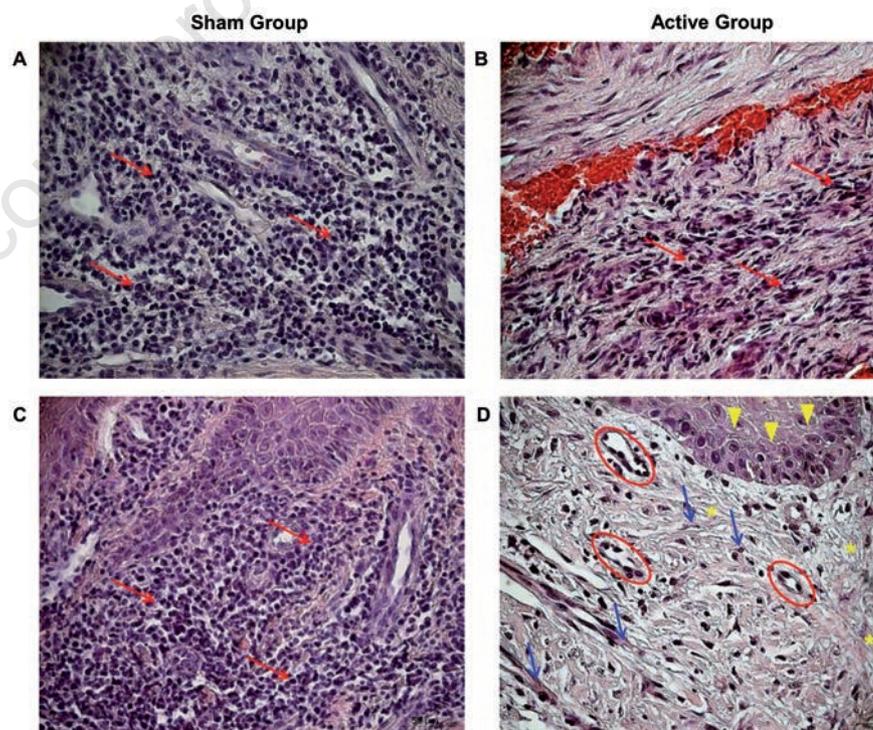

Figure 3. Hematoxylin and Eosin staining of DFUs at 20X magnification. Sham Group at baseline (A) and after the treatment with non-functioning TMR® device (C): Red arrows indicate granulocytes and macrophages. Active Group at baseline (B) and after the treatment with functioning TMR® device (D): yellow head arrows indicate a layer of cuboidal epithelial cells, red circles point to endothelial cells, blue arrows indicate fibroblasts, and yellow asterisks point to collagen fibers.

fibroblasts (blue arrows, Figure 3D), and endothelial cells (red circles, Figure 3D) were observable in the dermal layer (black bars in Figure 4B). Furthermore, in Active Group after 15-day treatment with functioning TMR® device few non-phagocytic cells such as lymphocytes, polymorphic nuclear cells (*i.e.,* granulocytes), and phagocytic cells such as macrophage were present (black bars in Figure 4B).

Real-time PCR array analysis

The principal molecules involved in the wound healing process were investigated by means of a real-time PCR array analysis. In particular, ECM components, cellular adhesion proteins, remodeling enzymes, cytoskeleton proteins, inflammatory cytokines, and growth factors were examined. Regarding ECM components, patients treated with Active TMR® showed a greater expression of collagens compared to patients treated with non-functioning TMR® device. The most significant increase is related to collagen type I (COL1A1 and COL1A2) and vitronectin (VTN) mRNA relative expression (Figure 5A). Interesting in cellular adhesion proteins profile is the expression of integrin alpha 1 (ITGA1) and integrin beta 3 (ITGB3), involved in vasculogenesis and focal adhesion process, respectively. Patients of Active Group showed a greater expression of ITGA1 and ITGB3 compared to those of Sham Group

(Figure 5B). Concerning remodeling enzymes, all examined matrix metalloproteinases (MMPs) displayed an important increase in transcription in case of treatment with PEMFs (Figure 5C). The same trend is observed in cytoskeleton proteins such as actins (ACTA2 and ACTC1) (Figure 5D).

The analysis of inflammatory cytokines reveals that patients treated with functioning TMR® device exhibited a greater expression of the anti-inflammatory interleukin (IL) 10 and a lesser expression of pro-inflammatory cytokines (black bars,

Figure 6A). Moreover, they showed high levels of growth factors transcripts, such as fibroblast growth factor (FGF) 2, FGF10, platelet-derived growth factor A (PDGFA), transforming growth factor (TGF) A, TGFB1, and vascular endothelial growth factor (VEGF) (black bars, Figure 6B). On the contrary, the subjects of Sham Group revealed greater expression of pro-inflammatory cytokines (white bars, Figure 6A) and tumor necrosis factor (TNF) (white bars, Figure 6B) typical of an inflammatory condition.
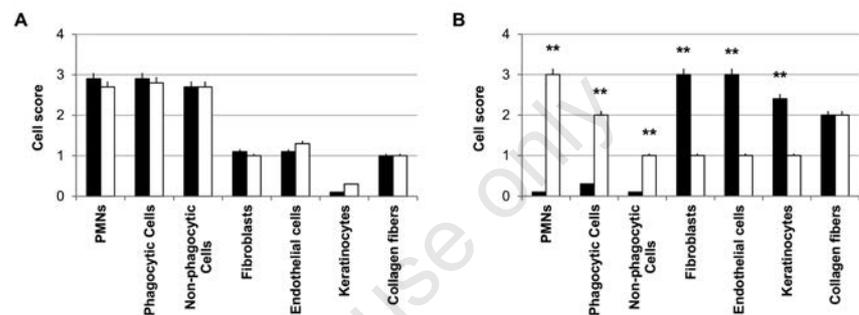

Figure 4. Histomorphometric analysis of biopsies from Sham Group (white bars) and Active Group (black bars): A) at baseline; B) after two week of TMR® treatment. PMNs are polymorphic nuclear cells, *i.e.* granulocytes; phagocytic cells include macrophages and monocyte-derived giant cells; non-phagocytic cells include lymphocytes, plasma cells and mast cells. Cells were scored as absent (score 0), scarcely present (score 1), present (score 2), and abundantly present (score 3). A *t*-test was used to determine significant differences (P<0.05): *P<0.05 and **P<0.01.
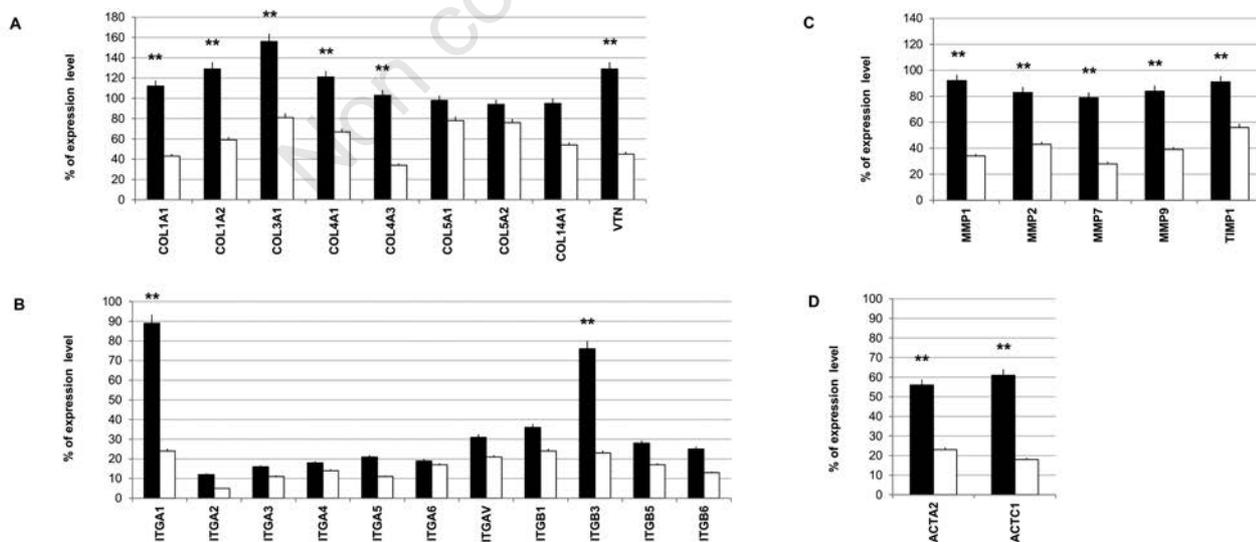

Figure 5. Real-time PCR array analysis: A) ECM components; B) cellular adhesion proteins; C) remodeling enzymes; D) cytoskeleton proteins. The results are reported as % of expression level of each target gene in post-treatment samples compared to pre-treatment samples in Sham Group (white bars) and Active Group (black bars). A *t*-test was used to determine significant differences (P<0.05): *P<0.05 and **P<0.01.

Discussion

Many different forms of extracellular signaling cues are used during wound healing to generate pattern and organization.[20-22] An understanding of these natural signals provides us with a basis for mimicking and optimizing them.

The healing process can actually be positively or negatively affected by a number of endogenous or exogenous factors, which may promote or hamper the repair of a chronic lesion, as an increasing number of published evidences demonstrates. As an example of this, platelet-derived growth factors and smoke have been proved to act on opposite ways in the same healing context.[23,24] Recently, PEMFs therapy has been used successfully as regenerative system in the management of chronic wounds.[13] The mechanisms by which the PEMFs improve healing are not known, making it difficult to substantiate use of any specific form of PEMFs and preventing optimization of treatments. The mechanisms of the action of TMR® on biological systems are still under investigation but the hypothesis are based on the physic of nonlinear dynamic processes. The efficacy of TMR® is assumed to be based on the interaction between magnetic fields and biologic processes. A mechanism

of electrical charges transport along macromolecules, which can be stimulated by weak magnetic fields pulsating at given resonant frequencies, has been identified. This mechanism can regulate metabolic processes, producing a healing effect on tissue lesions. TMR® delivers magnetic fields that pulsate only at tissue-specific frequencies, insofar stimulating and accelerating healing processes.[25] For this purpose, we have already performed an *in vitro* study with dermal-like tissues to investigate the effects of TMR® magnetic fields on skin remodeling.[15] In the current study, we tested these PEMFs properties *in vivo* on consecutive Type-2 diabetic patients. After 15 days of treatment with TMR®, we investigated the ability of PEMFs to induce both proliferation and migration of fibroblasts. After a lesion, these events are essential for tissue defect reconstitution, as fibroblasts are required to generate the granulation tissue, the temporary connective substitute of the original tissue, which in a later phase will evolve into the definitive scar.[25-28] The histological and histomorphometric analysis of DFUs treated with TMR® indicated a change in cell population after treatment with PEMFs. In particular, it was observed a greater presence of fibroblasts and endothelial cells with a reduction of cells involved in inflammatory process. The

ECM composition was investigated through the gene expression profile analysis of the principal molecules involved in wound healing process. TMR® led to a concomitant increase in MMPs, collagens and integrins expression in treated DFUs. Our results showed, in case of treatment with TMR®, an increase in expression of ITGB3, an integrin involved in focal adhesions,[29-31] confirming an improvement in cell migration, and then in wound healing process. In addition, TMR® increases the expression of ITGA1 and VEGF, both involved in the process of angiogenesis by facilitating endothelial cell migration and proliferation.[32-34] At the same time, collected data demonstrate that TMR® treatment produced a reduction in pro-inflammatory interleukins expression and an increase in growth factors expression. This is in agreement with a previous study of our group, in which we investigated the histological features of neuropathic DFUs. We demonstrated that removing the causes of the chronic pro-inflammatory state changing the histology of the ulcers and promoting a faster healing of the lesions.[20] This is in line with previous findings, all in chronic DFU models, who correlated the persistence of inflammatory cells with a low-intensity inflammatory state that creates a vicious cycle that 'freeze' the lesions in a non-evolutive condition, thus delaying or even impeding wound healing.[35-37]

In conclusion, our data suggest that TMR® magnetic fields may act reducing the inflammatory state, triggering a chain of events that promotes the shifting of the lesion towards the proliferative phase. The clinical correlates of the activity of TMR® demonstrated a more frequent and faster healing of DFUs; while the absence of side effects confirms the very positive safety profile of this approach to wound healing.
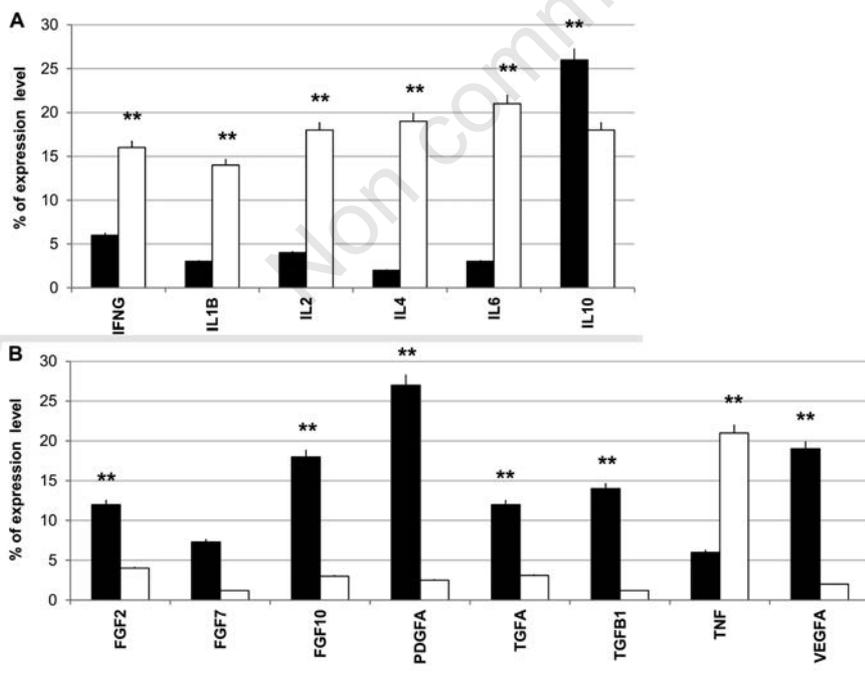

Figure 6. Real-time PCR array analysis: A) inflammatory cytokines; B) growth factors. The results are reported as % of expression level of each target gene in post-treatment samples compared to pre-treatment samples in both Sham Group (white bars) and Active Group (black bars). A *t*-test was used to determine significant differences (P<0.05): *P<0.05 and **P<0.01.

References

1. Lamers ML, Almeida ME, Vicente-Manzanares M, Horwitz AF, Santos MF. High glucose-mediated oxidative stress impairs cell migration. PLoS One 2011;6: e22865.
2. Bowling FL, Rashid ST, Boulton AJ. Preventing and treating foot complications associated with diabetes mellitus. Nat Rev Endocrinol 2015;11:606-16.
3. Berlanga-Acosta J, Schultz GS, López-Mola E, Guillen-Nieto G, García-Siverio M, Herrera-Martínez L. Glucose toxic effects on granulation tissue productive cells: the diabetics' impaired healing. Biomed Res Int 2013;2013:256043.

4. Gardin C, Ferroni L, Lancerotto L, Vindigni V, Rigo C, Roman M, et al. Nanoparticle therapies for wounds and ulcer healing. In: Kumar A, Mansour HM, Friedman A, Blough ER, Editors. Nanomedicine in drug deliver. CRC Press, Boca Raton: 2013; p. 143-186.

5. Wilbek TE, Jansen RB, Jørgensen B, Svendsen OL. The diabetic foot in a multidisciplinary team setting. Number of amputations below ankle level and mortality. Exp Clin Endocrinol Diabetes 2016;124:535-40.

6. Vouillermet J, Bourron O, Gaudric J, Lermusiaux P, Millon A, Hartemann A. Lower-extremity arterial revascularization: Is there any evidence for diabetic foot ulcer-healing? Diabetes Metab 2016;42:4-15.

7. Piaggesi A, Coppelli A, Goretti C, Iacopi E, Mattaliano, C. Do you want to organize a multidisciplinary diabetic foot clinic? We can help. Int J Low Extrem Wounds 2014;13:363-70.

8. Noor S, Zubair M, Ahmad J. Diabetic foot ulcer - A review on pathophysiology, classification and microbial etiology. Diabetes Metab Syndr 2015;9:192-9.

9. Yazdanpanah L, Nasiri M, Adarvishi S. Literature review on the management of diabetic foot ulcer. World J Diabetes 2015;6:37-53.

10. Cañedo-Dorantes L, García-Cantú R, Barrera R, Méndez-Ramírez I, Navarro VH, Serrano G. Healing of chronic arterial and venous leg ulcers through systemic effects of electromagnetic fields. Arch Med Res 2002;33:281-9.

11. Callaghan MJ, Chang EI, Seiser N, Aarabi S, Ghali S, Kinnucan ER, et al. Pulsed electromagnetic fields accelerate normal and diabetic wound healing by increasing endogenous FGF-2 release. Plast Reconstr Surg 2008;121:130-41.

12. Mulder G, Tenenhaus M, D'Souza GF. Reduction of diabetic foot ulcer healing times through use of advanced treatment modalities. Int J Low Extrem Wounds 2014;13:335-46.

13. Abbruzzese L, Iacopi E, Coppelli A, Bonino G, Goretti C, Piaggesi A. Safety and effectiveness of therapeutic magnetic resonance in the management of postsurgical lesion of the diabetic foot. Int J Low Extrem Wounds 2015;14:4-10.

14. Mani R; Margolis DJ, Shukla V, Akita S, Lazarides M, Piaggesi A, et al. Optimizing technology use for chronic lower-extremity wound healing: A consensus document. Int J Low Extrem Wounds 2016;15:102-19.

15. Ferroni L, Bellin G, Emer V, Rizzuto R, Isola M, Gardin C, et al. Treatment by Therapeutic Magnetic Resonance (TMR®) increases fibroblastic activity and keratinocyte differentiation in an in vitro model of 3D artificial skin. J Tissue Eng Regen Med 2017;11:1332-42.

16. Piaggesi A, Sambataro M, Nicoletti C, Goretti C, Lacopi E, Coppelli A. Safety and effectiveness of therapeutic magnetic resonance in diabetic foot ulcers: a prospective randomized controlled trial. J Wound Care 2016;25 704-11.

17. Bakker K, Apelqvist J, Lipsky BA, Van Netten JJ. International Working Group on the Diabetic Foot. The 2015 IWGDF guidance documents on prevention and management of foot problems in diabetes: development of an evidence-based global consensus. Diabetes Metab Res Rev 2016;32(S1):2-6.

18. Piaggesi A, Baccetti F, Rizzo L, Romanelli M, Navalesi R, Benzi L. Sodium carboxyl-methyl-cellulose dressings in the management of deep ulcerations of diabetic foot. Diabet Med 2001;18:320-4.

19. Piaggesi A, Macchiarini S, Rizzo L, Palumbo F, Tedeschi A, Nobili LA, et al. An off-the-shelf instant contact casting device for the management of diabetic foot ulcers: a randomized prospective trial versus traditional fiberglass cast. Diabetes Care 2007;30:586-90.

20. Piaggesi A, Viacava P, Rizzo L, Naccarato G, Baccetti F, Romanelli M, et al. Semiquantitative analysis of the histopathological features of the neuropathic foot ulcer: effects of pressure relief. Diabetes Care 2003;26:3123-8.

21. Xue M, Jackson CJ. Extracellular matrix reorganization during wound healing and its impact on abnormal scarring. Adv Wound Care (New Rochelle) 2015;4: 119-36.

22. Briquez PS, Hubbell JA, Martino MM. Extracellular matrix-inspired growth factor delivery systems for skin wound healing. Adv Wound Care (New Rochelle) 2015;4:479-89.

23. Marrelli M, Tatullo M. Influence of PRF in the healing of bone and gingival tissue. Clinical and histological evaluations. Eur Rev Med Pharmacol Sci 2013;17:1958-62.

24. Tatullo M, Gentile S, Paduano F, Santacroce L, Marrelli M. Cross-talk between oral and general health status in e-smokers. Medicine (Baltimore) 2016;95:e5589.

25. Sawicka KM, Seeliger M, Musaev T, Macri LK, Clark RA. Fibronectin interaction and enhancement of growth factors: Importance for wound healing. Adv Wound Care (New Rochelle) 2015;4: 469-78.

26. Brizhik L, Zavan B, Fermi E. The working principle of magnetic resonance therapy. Cornell Univ Library 2015; arXiv:1509.04475 [physics.med-ph]. Available from: https://arxiv.org/abs/1509.04475

27. Cortivo R, Vindigni V, Iacobellis L, Abatangelo G, Pinton P, Zavan B. Nanoscale particle therapies for wounds and ulcers. Nanomedicine (Lond) 2010; 5:641-56.

28. Laverdet B, Danigo A, Girard D, Magy L, Demiot C, Desmoulière A. Skin innervation: important roles during normal and pathological cutaneous repair. Histol Histopathol 2015;30:875-92.

29. Isakson M, de Blacam C, Whelan D, McArdle A, Clover, AJ. Mesenchymal stem cells and cutaneous wound healing: Current evidence and future potential. Stem Cells Int 2015;2015:831095.

30. Bauer SM, Bauer RJ, Velazquez OC. Angiogenesis, vasculogenesis, and induction of healing in chronic wounds. Vasc Endovascular Surg 2005;39:293-306.

31. Collins C, Nelson WJ. Running with neighbors: coordinating cell migration and cell-cell adhesion. Curr Opin Cell Biol 2015;36:62-70.

32. Koivisto L, Heino J, Häkkinen L, Larjava H. Integrins in wound healing. Adv Wound Care (New Rochelle) 2014;3: 762-83.

33. Longmate WM, Dipersio CM. Integrin regulation of epidermal functions in wounds. Adv Wound Care (New Rochelle) 2014;3:229-46.

34. Witmer AN, Vrensen GF, Van Noorden CJ, Schlingemann RO. Vascular endothelial growth factors and angiogenesis in eye disease. Prog Retin Eye Res 2003;22: 1-29.

35. Zavan B, Vindigni V, Vezzù K, Zorzato G, Luni C, Abatangelo G, et al. Hyaluronan based porous nano-particles enriched with growth factors for the treatment of ulcers: a placebo-controlled study. J Mater Sci Mater Med 2009;20: 235-47.

36. Figallo E, Flaibani M, Zavan B, Abatangelo G, Elvassore N. Micro-patterned biopolymer 3D scaffold for static and dynamic culture of human fibroblasts. Biotechnol Prog 2007;23: 210-6.

37. Eming SA, Martin P, Tomic-Canic M. Wound repair and regeneration: mechanisms, signaling, and translation. Sci Transl Med 2014;6:265sr6.